The Astrophysical Journal, 831:193 (7pp), 2016 November 10 doi:10.3847/0004-637X/831/2/193

A SEARCH FOR VERY HIGH ENERGY GAMMA RAYS FROM THE MISSING LINK BINARY PULSAR J1023+0038 WITH VERITAS

E. Aliu[1], S. Archambault[2], A. Archer[3], W. Benbow[4], R. Bird[5], J. Biteau[6], M. Buchovecky[7], J. H. Buckley[3], V. Bugaev[3], K. Byrum[8], J. V Cardenzana[9], M. Cerruti[4], X. Chen[10,11], L. Ciupik[12], M. P. Connolly[13], W. Cui[14], H. J. Dickinson[9], J. D. Eisch[9], A. Falcone[15], Q. Feng[14], J. P. Finley[14], H. Fleischhack[11], A. Flinders[16], P. Fortin[4], L. Fortson[17], A. Furniss[18], G. H. Gillanders[13], S. Griffin[2], J. Grube[12], G. Gyuk[12], M. Hütten[11], N. Håkansson[10], J. Holder[19], T. B. Humensky[20], C. A. Johnson[6], P. Kaaret[21], P. Kar[16], N. Kelley-Hoskins[11], M. Kertzman[22], D. Kieda[16], M. Krause[11], M. J. Lang[13], A. Loo[20], G. Maier[11], S. McArthur[14], A. McCann[2], K. Meagher[23], P. Moriarty[13], R. Mukherjee[1], T. Nguyen[23], D. Nieto[20], A. O'Faoláin de Bhróithe[11], R. A. Ong[7], A. N. Otte[23], D. Pandel[24], N. Park[25], V. Pelassa[4], A. Petrashyk[20], M. Pohl[10,11], A. Popkow[7], E. Pueschel[5], J. Quinn[5], K. Ragan[2], P. T. Reynolds[26], G. T. Richards[23], E. Roache[4], C. Rulten[17], M. Santander[1], G. H. Sembroski[14], K. Shahinyan[17], A. W. Smith[27], D. Staszak[25], I. Telezhinsky[10,11], J. V. Tucci[14], J. Tyler[2], A. Varlotta[14], S. Vincent[11], S. P. Wakely[25], O. M. Weiner[20], A. Weinstein[9], A. Wilhelm[10,11], D. A. Williams[6], B. Zitzer[8], M. Chernyakova[28,29], and M. S. E. Roberts[30,31]

[1] Department of Physics and Astronomy, Barnard College, Columbia University, NY 10027, USA; ester.aliu.fuste@gmail.com
[2] Physics Department, McGill University, Montreal, QC H3A 2T8, Canada
[3] Department of Physics, Washington University, St. Louis, MO 63130, USA
[4] Fred Lawrence Whipple Observatory, Harvard-Smithsonian Center for Astrophysics, Amado, AZ 85645, USA
[5] School of Physics, University College Dublin, Belfield, Dublin 4, Ireland
[6] Santa Cruz Institute for Particle Physics and Department of Physics, University of California, Santa Cruz, CA 95064, USA
[7] Department of Physics and Astronomy, University of California, Los Angeles, CA 90095, USA
[8] Argonne National Laboratory, 9700 S. Cass Avenue, Argonne, IL 60439, USA
[9] Department of Physics and Astronomy, Iowa State University, Ames, IA 50011, USA
[10] Institute of Physics and Astronomy, University of Potsdam, D-14476 Potsdam-Golm, Germany
[11] DESY, Platanenallee 6, D-15738 Zeuthen, Germany
[12] Astronomy Department, Adler Planetarium and Astronomy Museum, Chicago, IL 60605, USA
[13] School of Physics, National University of Ireland Galway, University Road, Galway, Ireland
[14] Department of Physics and Astronomy, Purdue University, West Lafayette, IN 47907, USA
[15] Department of Astronomy and Astrophysics, 525 Davey Lab, Pennsylvania State University, University Park, PA 16802, USA
[16] Department of Physics and Astronomy, University of Utah, Salt Lake City, UT 84112, USA
[17] School of Physics and Astronomy, University of Minnesota, Minneapolis, MN 55455, USA
[18] Department of Physics, California State University—East Bay, Hayward, CA 94542, USA
[19] Department of Physics and Astronomy and the Bartol Research Institute, University of Delaware, Newark, DE 19716, USA
[20] Physics Department, Columbia University, New York, NY 10027, USA
[21] Department of Physics and Astronomy, University of Iowa, Van Allen Hall, Iowa City, IA 52242, USA
[22] Department of Physics and Astronomy, DePauw University, Greencastle, IN 46135-0037, USA
[23] School of Physics and Center for Relativistic Astrophysics, Georgia Institute of Technology, 837 State Street NW, Atlanta, GA 30332-0430, USA; gtrichards@gatech.edu
[24] Department of Physics, Grand Valley State University, Allendale, MI 49401, USA
[25] Enrico Fermi Institute, University of Chicago, Chicago, IL 60637, USA
[26] Department of Physical Sciences, Cork Institute of Technology, Bishopstown, Cork, Ireland
[27] University of Maryland, College Park/NASA GSFC, College Park, MD 20742, USA
[28] School of Physical Sciences, Dublin City University, Dublin 9, Ireland; masha.chernyakova@dcu.ie
[29] Dublin Institute for Advanced Studies, 31 Fitzwilliam Place, Dublin 2, Ireland
[30] New York University Abu Dhabi, P.O. Box 129188 Saadiyat Island, Abu Dhabi, UAE; malloryr@gmail.com
[31] Eureka Scientific, 2452 Delmer Street, Suite 100, Oakland, CA 94602, USA

Received 2016 February 18; revised 2016 July 20; accepted 2016 August 26; published 2016 November 8

ABSTRACT

The binary millisecond radio pulsar PSR J1023+0038 exhibits many characteristics similar to the gamma-ray binary system PSR B1259–63/LS 2883, making it an ideal candidate for the study of high-energy nonthermal emission. It has been the subject of multiwavelength campaigns following the disappearance of the pulsed radio emission in 2013 June, which revealed the appearance of an accretion disk around the neutron star. We present the results of very high energy (VHE) gamma-ray observations carried out by the Very Energetic Radiation Imaging Telescope Array System before and after this change of state. Searches for steady and pulsed emission of both data sets yield no significant gamma-ray signal above 100 GeV, and upper limits are given for both a steady and pulsed gamma-ray flux. These upper limits are used to constrain the magnetic field strength in the shock region of the PSR J1023+0038 system. Assuming that VHE gamma rays are produced via an inverse Compton mechanism in the shock region, we constrain the shock magnetic field to be greater than ∼2 G before the disappearance of the radio pulsar and greater than ∼10 G afterward.

Key words: binaries: general – gamma rays: general – pulsars: general – pulsars: individual (PSR J1023+0038)

1. INTRODUCTION

Radio millisecond pulsars (MSPs) are old neutron stars that have been spun up to millisecond periods via accretion of material from a companion star in a low-mass X-ray binary (LMXB; Alpar et al. 1982). In the past few years, new MSP discoveries have taken place at a greatly elevated rate due to searches for radio pulsars in unassociated *Fermi*-LAT-detected gamma-ray sources (Ray et al. 2012). This new population of MSPs has enriched the known diversity of binary MSP companions. This is especially true for eclipsing systems, which were rarely seen outside of globular clusters: the "black widows" with very low mass ($M \ll 0.1\ M_{\odot}$) companions and "redback" systems with more massive ($M_c \gtrsim 0.1\ M_{\odot}$), non-degenerate companions (Roberts 2011). Some of these redbacks have been observed to transition between LMXB and MSP states, providing the first direct observational evidence to support the theory of the MSP formation mechanism. There are now three systems where transitions have been observed: PSR J1023+0038 (Archibald et al. 2009) and XSS 12270–4859 (Bassa et al. 2014; Roy et al. 2015) in the Galactic plane, and PSR J1824–2452I (Papitto et al. 2013), located in the globular cluster M28. Additionally, it has recently been suggested that the galactic binary 1RXS J154439.4–112820 may also be a transitional system (Bogdanov 2015).

Very high energy (VHE) gamma-ray emission ($E > 100$ GeV) from binaries containing MSPs has been predicted to occur through diverse mechanisms. Harding et al. (2005) propose that leptons accelerated above the polar cap can produce inverse Compton or curvature radiation emission that could potentially be identified as gamma-ray pulsations at energies up to and above 100 GeV, similar to what has been observed from the young Crab pulsar (Aliu et al. 2008, 2011). Additionally, leptons could be accelerated at the shock that appears as a result of the interaction between the pulsar wind and material ablated off of the companion. These leptons could then radiate VHE gamma rays via inverse Compton scattering, which could be modulated with the binary orbital period. This emission scenario is thought to occur in the VHE-detected binary system PSR B1259–63/LS 2883, a radio pulsar in a ∼3.4 yr orbit around a massive, luminous Be star (Aharonian et al. 2005).

The theory of VHE gamma-ray emission from PSR B1259–63 (Tavani et al. 1994) was first explored in the context of the original Black Widow Pulsar system (Arons & Tavani 1993), which is a binary comprising the 1.6 ms pulsar PSR B1957+20 in a 9.2 hr orbit around a ∼0.02 $M_{\odot}$ companion. However, no VHE emission has been detected from the Black Widow (Otte 2007). Searches for VHE emission from several globular clusters have been undertaken, since they are known to contain many of these eclipsing binary systems. Recently, the High Energy Stereoscopic System (H.E.S.S.) has detected VHE emission from the direction of the cluster Terzan 5 (Abramowski et al. 2011), which is especially rich in eclipsing binary systems among globular clusters (Ransom 2008, p. 291). This emission is thought to originate in a bow shock region where interactions between leptons from MSP winds and the galactic medium occur (Bednarek & Sobczak 2014). However, searches for VHE emission from the globular clusters 47 Tuc (Aharonian et al. 2009), M5, M15 (McCutcheon et al. 2009), and M13 (Anderhub et al. 2009; McCutcheon 2012) have revealed no such emission. The aforementioned eclipsing binary systems in globular clusters can be seen as smaller-scale versions of PSR B1259–63, because their more massive, nearly Roche-lobe-filling companions provide much larger targets and more copious seed photons for inverse Compton scattering than companions of black widows. With the discovery of nearby redbacks in the Galactic field, it is thought that a single, energetic Galactic-field redback could be brighter at VHE energies than the combined emission from many eclipsing systems in a distant cluster (Roberts 2011).

PSR J1023+0038 is a redback system containing a 1.69 ms MSP in a 4.8 hr orbit around a G star with a mass of ∼0.2 $M_{\odot}$ (Archibald et al. 2009). PSR J1023+0038 was selected as a promising candidate for VHE observations with the Very Energetic Radiation Imaging Telescope Array System (VERITAS) based on three parameters thought to be responsible for the VHE emission from PSR B1259–63: the high spin-down luminosity of the pulsar, the presence of an intense target photon field for inverse Compton scattering provided by the companion, and the relatively small distance from Earth. Although the optical luminosity of the companion in PSR J1023+0038 is a factor of $\sim 10^4$ less than that for the companion of PSR B1259–63, this discrepancy is possibly compensated by the much smaller distance separating the pulsar and its companion in PSR J1023+0038, potentially making the energy density of seed photons at the shock comparable for the two systems. However, the PSR B1259–63 system has a circumstellar disk that the pulsar passes through at periastron (Wex et al. 1998), though PSR J1023+0038 shows no evidence of such a disk.

While the actual VHE emission will depend on the details of the flow and the magnetic field at the shock, the inverse Compton emission should roughly scale as $F_{\rm IC} \propto f\,(\dot{E}/d^2)u_{\rm ph}$, where d is the distance to the binary, $u_{\rm ph} \sim (R_c/R_s)^2\sigma T_c^4/c$ is the photon energy density at the shock, R_c is the radius of the companion, R_s is the radius of the shock measured from the companion, and f is a geometrical factor representing the fraction of the pulsar wind involved in the shock. If the shock region of PSR J1023+0038 (and by extension other redbacks and black widows) is very near the surface of the companion, as proposed by Bogdanov et al. (2011), then $R_c/R_s \sim 1$, and f is related to the angle subtended by the companion in the pulsar sky. In the extreme case of a shock only near the surface of the companion, f is approximately 0.01 if the pulsar wind is isotropic, and f is approximately 0.07 if the wind is confined to the equatorial plane. Based on this simple estimation, the expected TeV flux from PSR J1023+0038 would be on the order of $\sim 0.1f$ that of PSR B1259–63 near periastron, where it has an observed flux $F\,(E > 1\ \text{TeV}) \sim 10^{-11}\ \text{cm}^{-2}\ \text{s}^{-1}$ (H.E.S.S. Collaboration et al. 2013). We note that PSR J1023+0038 was selected for observations before the publication of the revised estimates for the distance and spin-down power given in Deller et al. (2015), in which case the estimated TeV flux would have been closer to $1f$ that of PSR B1259–63.

Orbitally modulated X-ray emission has been observed from PSR J1023+0038, suggesting that the system contains shocked material (Archibald et al. 2010), and the observed radio eclipses suggest that the shock region may be quite large. Tam et al. (2010) found strong evidence of gamma-ray emission from the direction of PSR J1023+0038 in the high-energy (HE; 100 MeV $\lesssim E \leqslant$ 100 GeV) gamma-ray band using *Fermi*-LAT data. Given the observed steep spectrum of this emission ($\Gamma \sim 3$), the authors suggest that the gamma rays

likely originate from the pulsar magnetosphere rather than the intrabinary shock. Indeed, Archibald et al. (2013) have reported a hint of pulsed HE gamma-ray emission from the pulsar magnetosphere with a statistical significance of 3.7σ.

A sudden change of state in PSR J1023+0038 was reported to have occurred in 2013 June after the pulsed radio emission from the MSP was no longer detected (Stappers et al. 2013), and optical evidence for an accretion disk in the system was found for the first time since 2001 December (Szkody et al. 2003; Halpern et al. 2013). The X-ray emission increased only moderately (Kong 2013; Patruno et al. 2013), implying that accretion may still be inhibited due to the influence of the pulsar magnetosphere, although low-level X-ray pulsations, thought to be powered by accretion, have been detected (Archibald et al. 2014). All of this new behavior coincided with a fivefold increase in the HE gamma-ray flux from PSR J1023+0038 (Stappers et al. 2014).

The similarities between PSR J1023+0038 and PSR B1259–63/LS 2883 motivated the first VERITAS observations of the PSR J1023+0038 in 2010. Follow-up observations took place after the system was reported to have transitioned to an accretion/LMXB state in 2013, prompted by the substantial increase in flux in the HE gamma-ray band observed with the *Fermi*-LAT. Here we report the results of these observations of PSR J1023+0038, the first ever made in the VHE band, covering the two different states of this exceptional transitional object. After describing the observations (Section 2), the analysis and results are presented (Section 3), including searches for steady emission from the binary and pulsed emission from the pulsar magnetosphere. In the final section we provide a simple spectral model to interpret and discuss the results (Section 4).

2. VHE GAMMA-RAY OBSERVATIONS

The VERITAS is a ground-based array of four imaging atmospheric Cerenkov telescopes operating at the Fred Lawrence Whipple Observatory in southern Arizona, USA. It was designed to explore the universe in VHE gamma rays in the energy range from ~85 GeV to above 30 TeV. Brief Cerenkov light flashes from gamma-ray- and cosmic-ray-initiated air showers are focused by 12 m reflectors onto cameras comprising 499 photomultiplier tubes located in the focal plane of each telescope, giving a $3.^{\circ}5$ diameter field of view. The angular resolution of the array (68% containment) reaches $0.^{\circ}08$ per gamma-ray photon candidate, with a sensitivity to detect a point source at the 5σ level with 1% of the Crab Nebula flux above 300 GeV and at a 20° zenith angle in approximately 25 hr. For a review of the detector, see Holder et al. (2006, 2008).

The first observations of PSR J1023+0038 were made by VERITAS between 2010 December 8 and 2011 February 25 when the system was in the radio MSP state, resulting in 20 hr of live time available for analysis after data quality selection. Further observations took place in 2013 December for a total of 10 hr of live time coinciding with the newly reported accretion/LMXB state of the system. The two sets of data were recorded in two different configurations of the VERITAS array: 2009 August to 2012 July, with the original cameras and electronics; and 2012 August to present, following an upgrade to the telescope cameras and the trigger system (for details, see Kieda et al. 2013). Data were taken on clear and moonless nights in *wobble* observation mode, in which the telescope pointing is offset by $0.^{\circ}5$ from the position of PSR J1023+0038, alternating between the four cardinal directions to allow simultaneous accumulation of data and background (Fomin et al. 1994). The data span the zenith angle range of 31°–39°.

3. VERITAS ANALYSIS AND RESULTS

3.1. Analysis

The data are analyzed with a standard VERITAS software pipeline for reconstructing the primary parameters of the gamma rays (see, e.g., Acciari et al. 2008) and cross-checked using an independent calibration and analysis software package. The images are first flat-fielded by recording the response of the cameras to a pulsed UV LED system (Hanna et al. 2010). The images are cleaned to remove contamination by night-sky background (Daniel 2008) and parameterized by their principal moments (Hillas 1985). Arrival directions and impact distances are estimated by analyzing the orientation of shower images in different telescopes (Hofmann et al. 1999). Background estimation is achieved by comparison of the parameters of the recorded events with those computed in Monte Carlo gamma-ray simulations (Krawczynski et al. 2006).

3.2. Search for a Steady Signal

A search for a VHE gamma-ray excess signal from the direction of PSR J1023+0038 is carried out independently for the two states of the system observed with VERITAS. None of these searches yield a significant excess over the estimated background from the location of PSR J1023+0038. Upper limits (ULs) on the integral flux above 300 GeV from PSR J1023+0038 for each state are set. The approach of Rolke et al. (2005) is used to determine these ULs at the 95% confidence level (CL) assuming a power-law source spectrum with a photon index of $\Gamma = 2.5$. The 95% CL ULs are 8.1×10^{-13} and 9.6×10^{-13} cm^{-2} s^{-1}, respectively. For more information, refer to Table 1.

Given that PSR J1023+0038 shows orbital modulation in the X-ray band, a search for VHE gamma-ray emission at different orbital phases is also performed. The data are divided into 10 phase bins and undergo the same standard analysis as described in Section 3.1. For both the radio MSP state and the accretion/LMXB state, no significant excess is found in any of the orbital bins.

3.3. Search for Pulsations

A search for pulsed gamma-ray emission in the VHE band from the position of PSR J1023+0038 is performed in two parts using data recorded by VERITAS during time periods in which the radio MSP was active and after the disappearance of the MSP and re-emergence of an accretion disk (accretion/LMXB state). After applying the background rejection and data quality cuts outlined in Section 3.1, photon arrival times are barycentered and phase-folded to the pulsar period in the `Tempo2` software package (Hobbs et al. 2006) using a PSR J1023+0038 Jodrell Bank ephemeris derived from radio data spanning MJD 55,540 to 55,644 (2010 December 10 to 2011 March 24). Details on the creation of the Jodrell Bank radio ephemeris can be found in Section 3 of Archibald et al. (2013). Since the pulsar ephemeris used is no longer valid during the accretion/LMXB phase, only results from the radio MSP state are shown. The phase-folded light curve of PSR J1023+0038

Table 1
VERITAS Analysis Results for the Location of PSR J1023+0038 for Each of the Two Different Binary States

Binary State	On Events	Off Events	α	Excess Events	LiMa Significance	95% CL Flux UL ($cm^{-2}\,s^{-1}$)	95% CL Flux UL (Flux Units) ($erg\,cm^{-2}\,s^{-1}$)
Radio MSP	287	1815	0.17	−15.5	−0.8	8.1×10^{-13}	5.8×10^{-13}
Accretion/LMXB	72	422	0.17	1.7	0.2	9.6×10^{-13}	6.9×10^{-13}

Note. The parameter α indicates the ratio of the on- to off-source region exposure, and the LiMa significance is calculated using Equation (17) in Li & Ma (1983).

is shown in Figure 1. De Jager's *H*-test is employed to compute *H* statistics that reflect the likelihood of the presence of a periodic signal in the light curve (de Jager 1989). Application of the *H*-test does not yield any evidence of periodicity in the VHE gamma-ray data. Subsequently, integral flux limits above an energy threshold of 166 GeV are computed with the method of de Jager (1994) assuming a pulsar duty cycle of 10%, a Gaussian pulse shape, and a spectral index of 3.8 (the same index measured by VERITAS for the Crab pulsar in Aliu et al. 2011). *H* statistics and integral VHE flux limits are given in Table 2.

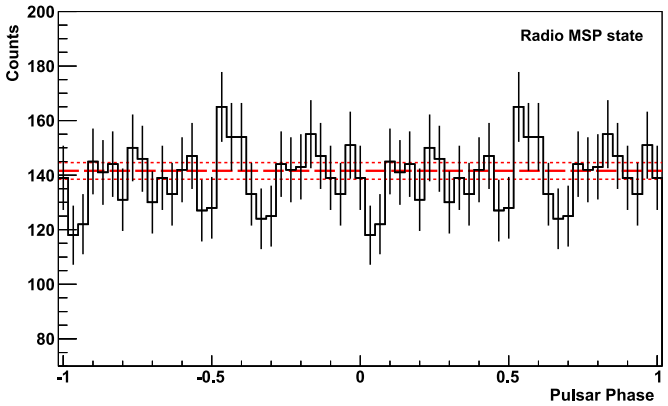

Figure 1. Light curve of events phase-folded with the Jodrell Bank radio ephemeris for the radio MSP state. The light curve shows two pulsar periods and contains 30 bins per period. The dashed and dotted red lines represent the average number of counts and error on the average, respectively.

4. DISCUSSION AND CONCLUSION

During the past decade, PSR J1023+0038 has been intensively investigated in different energy bands. In this paper we have reported two sets of VERITAS observations, taken during the radio MSP state and the accretion/LMXB state, that have both yielded upper limits on a VHE gamma-ray flux. While the beginning of the accretion phase was marked by a sharp rise of the luminosity in both X-rays and HE gamma rays as observed by *Swift* and *Fermi*-LAT (Stappers et al. 2013; Takata et al. 2014), the source was not detected by VERITAS. In the following, we discuss the constraints that can be placed on the physical properties of PSR J1023+0038 with the VERITAS upper limits. First, we will discuss the system when PSR J1023+0038 exhibited detectable radio pulses, and then we will investigate what changed after the reappearence of the accretion disk.

4.1. Millisecond Pulsar Phase

During the MSP phase, radio emission from PSR J1023 +0038 was characterized by highly frequency-dependent eclipses at superior conjunction accompanied by short, irregular eclipses at all orbital phases (Archibald et al. 2009). Assuming a pulsar mass $M = 1.4M_{\odot}$ and an orbital inclination $i \sim 46°$, it has been shown that the line of sight between the pulsar and Earth does not intersect the Roche lobe of the companion at any point of the orbit (Archibald et al. 2009). Therefore, the eclipses must be caused by material driven off the surface of the companion by the impinging pulsar wind.

The *V* magnitude of the system is orbitally modulated, reaching a minimum during the inferior conjunction of the companion star (Thorstensen & Armstrong 2005). Such behavior is consistent with a Roche-lobe-filling companion near $T_{\rm eff} = 5650$ K being illuminated by a pulsar with an isotropic luminosity of $\sim 2L_{\odot}$.

Orbitally modulated X-ray emission from PSR J1023+0038 was observed by the *XMM-Newton* and *Chandra* X-ray observatories in 2004, 2008, and 2010 (Homer et al. 2006; Archibald et al. 2010; Bogdanov et al. 2011). In Archibald et al. (2010), it is shown that in the energy range 0.25–2.5 keV, the X-ray emission is also modulated at the 1.6 ms rotational period of the MSP with a mean-squared pulsed fraction of 0.11 (2). X-ray emission observed with *Swift*-XRT in the 0.3–8 keV energy range suggests a dominant nonthermal synchrotron component originating at the intrabinary shock. In the case of a magnetically dominated wind (with a ratio of magnetic energy to kinetic energy $\sigma \gg 1$), the shock should occur in a relatively strong magnetic field ($B \sim 40$ G) due to the small separation between the pulsar and the companion (Bogdanov et al. 2011). In Bogdanov et al. (2011) it is shown that the depth and duration of the X-ray eclipses imply that the intrabinary shock is localized close to the L1 Lagrangian point and has a size of about $R \sim 5 \times 10^{10}$ cm. *NuSTAR* has detected a power law throughout the 3–79 keV band with an estimated luminosity of 7.4×10^{32} erg s^{-1} (Tendulkar et al. 2014). If the estimate of the shock size by Bogdanov et al. (2011) is correct, then a very large fraction of the energy in the shocked portion of the wind must be converted to X-ray emission, which supports the high-σ scenario. In Archibald et al. (2010) it is also noted that emission from the pulsar magnetosphere can contribute to the nonthermal X-ray emission, but the orbital modulation indicates that this component is not dominant.

In addition to the aforementioned nonthermal emission, there also is a faint thermal component possibly originating from the hot polar caps of the pulsar and optically thin thermal plasma responsible for the radio eclipses. There is no evidence in X-ray data for a wind nebula associated with the pulsar. The observed X-ray luminosity in the 0.5–10 keV energy range of $L_{\rm X} \sim 10^{32}$ erg s^{-1} (assuming a distance of 1.4 kpc; Deller et al. 2012) is much less than the spin-down luminosity: $L_{\rm sd} \simeq 3.2 \times 10^{34}$ erg s^{-1} (Archibald et al. 2013).

The broadband spectrum of PSR J1023+0038 from X-rays to VHE gamma rays is shown in Figure 2. While the X-ray data can be described by synchrotron emission from relativistic electrons exhibiting a power law with an exponential cutoff

Table 2
H Statistic and Integral Pulsed VHE Flux Upper Limit Computed with the VERITAS Data for the Radio MSP State of PSR J1023+0038

PSR J1023+0038 State	*H* Statistic	95% CL Pulsed VHE Flux UL (cm^{-2} s^{-1})	95% CL Pulsed VHE Flux UL (Flux Units; erg cm^{-2} s^{-1})
Radio MSP	0.50	1.5×10^{-12}	2.0×10^{-12}
Accretion/LMXB	...	...	...

Note. Due to the unavailability of a valid pulsar timing solution for the accretion/LMXB state, no *H* statistic or flux upper limit is given for VERITAS data collected during this state.

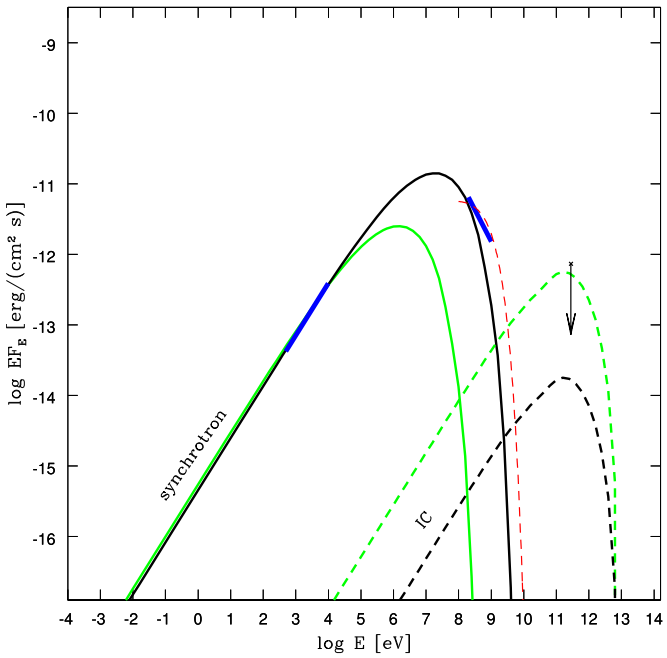

Figure 2. Broadband spectrum of PSR J1023+0038 during the MSP phase. Thick blue bars show the detection of the X-ray emission by *XMM-Newton* in 2008 (Archibald et al. 2010) and the *Fermi*-LAT GeV detection (Tam et al. 2010). The black solid line represents synchrotron emission in a 40 G magnetic field, and the black dashed line represents the component due to inverse Compton scattering of optical photons. The solid and dashed green lines represent those same components in the case of a 2 G magnetic field. The red dashed line represents a typical power-law model with an exponential cutoff spectrum of a GeV MSP. The arrow represents the VERITAS flux upper limit reported in this work.

spectral shape, $dN/dE \propto E^{-2.52}\exp(-E/E_{\rm cut})$, the GeV data are not readily fitted with the same component. However, since the X-ray and GeV gamma-ray data are not strictly contemporaneous, spectral variability cannot be ruled out. The situation is similar if the observed GeV emission is produced in the pulsar magnetosphere. The typical spectral shape of the GeV MSPs is a power law with an exponential cutoff (e.g., Espinoza et al. 2013); see the red dashed line in Figure 2 for a best fit to the *Fermi*-LAT data (Tam et al. 2010). This spectral shape is thought to be a result of curvature acceleration in a gap region in the magnetosphere (Harding et al. 2005). More data are needed to distinguish between a synchrotron or curvature radiation origin of the GeV emission, although neither predicts emission above 10 GeV.

Synchrotron photons can inverse Compton scatter on relativistic electrons and become VHE photons. The ratio of the total power radiated by the synchrotron radiation and by inverse Compton scattering by the same distribution of electrons is equal to $\eta = (dE/dt)_{\rm sync.}/(dE_e/dt)_{\rm IC}$. The value for η reaches a maximum in the Thomson limit in which $\eta_{\rm T} = \frac{B^2/8\pi}{U_{\rm rad}}$, where $U_{\rm rad}$ is the energy density of the synchrotron photons. It turns out that for PSR J1023+0038, the total energy of scattered photons is much smaller than the total energy of the synchrotron photons even in the Thomson limit where

$$\eta_{\rm T} \sim 600\frac{(B/40\ {\rm G})^2(R/5\times10^{10}\ {\rm cm})^2}{L/10^{32}\ {\rm erg\ s^{-1}}}. \quad (1)$$

An additional potential source of VHE emission is external inverse Compton scattering of soft photons from the optically bright companion with an effective temperature of $T = 5650$ K (Thorstensen & Armstrong 2005). This inverse Compton component is shown in Figure 2 as a black dashed line. Given the assumed value of the magnetic field, $B = 40$ G, the component lies well below the VHE flux upper limit. However, for a lower magnetic field strength, the difference between the peak flux values of the synchrotron and inverse Compton components will become smaller, allowing VERITAS observations to set a lower limit on the magnetic field strength. As shown by the green lines in Figure 2, the case of a 2 G magnetic field gives close to the peak inverse Compton flux allowed by the upper limit derived from the VERITAS data.

Note that for a 2 G magnetic field, $\eta_{\rm T}$ defined by Equation (1) is close to unity. However, X-ray photons will be upscattered in the Klein–Nishina regime, and in this case the total energy of scattered photons is much smaller than in the Thomson regime:

$$\eta_{\rm KN} = \frac{B^2/8\pi}{\frac{9}{32}U_{\rm rad}}\frac{\ln(\hbar\omega_0\gamma/m_ec)^2}{\gamma^2\hbar^2\omega_0^2/(m_ec^2)^2} \sim \eta_{\rm T}/2000 \quad (2)$$

for 1 keV photons scattered into the VHE band by electrons with $\gamma = 10^4$ (Longair 2011). Although lower-energy photons are scattered in the transition regime between the Thomson and Klein–Nishina regimes, their energy density is much lower than that of the X-ray photons, and so the self-scattering process is not important in this case either.

4.2. Accretion Phase

The reappearance of the accretion disk in 2013 June was accompanied by the disappearance of radio pulsations and an increase of the X-ray and HE gamma-ray luminosities. Accreting binary systems are not typically bright in the GeV domain. The only two binaries detected by *Fermi*-LAT in which the presence of an accretion disk is certain are Cyg X-3 and Cyg X-1 (Corbel et al. 2012; Malyshev et al. 2013), and in both cases the HE emission is not believed to come from the disk, but rather to be generated in the relativistic jet. The formation of a jet in PSR J1023+0038 has not been observed in VLBI imaging, although variable point-source emission has been seen (Deller et al. 2015). Further, it appears that the X-ray pulsations, indicating accretion onto the neutron star surface, are intermittent (Archibald et al. 2014). Therefore, it could be the case that, as discussed by Takata et al. (2014), Coti Zelati

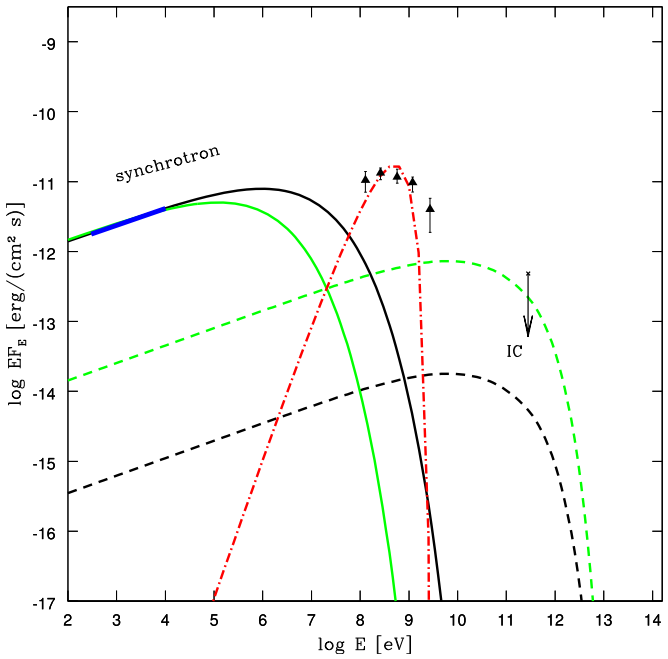

Figure 3. Broadband spectrum of PSR J1023+0038 after the reappearance of the accretion disk. The thick blue bar shows the X-ray emission detected by *Swift* in 2013 November (Takata et al. 2014). Black triangles represent the *Fermi*-LAT HE gamma-ray detection in 2013 (Takata et al. 2014). The arrow shows the VERITAS upper limit for the accretion/LMXB state, as reported in this work. Solid and dashed lines correspond to the synchrotron and inverse Compton emission coming from the shock for the case of a 10 G (green lines) and 80 G (black lines) magnetic field. The spectral signature of inverse Compton scattering of photons emitted by the accretion disk on the unshocked electrons is shown with a red dot-dashed line.

et al. (2014), Li et al. (2014), and Papitto & Torres (2015), the rotation-powered MSP is still at least partially active in PSR J1023+0038, and the complete disappearance of the pulsations is due to absorption by matter evaporating from the accretion disk. In this case, the principal differences from the radio MSP state discussed in the previous section would be (a) the presence of additional soft photons emitted by the accretion disk and (b) the shift of the shock closer to the pulsar due to the inward pressure of the disk.

The presence of additional photons from the accretion disk leads to an increase of the HE luminosity as a result of scattering of those photons on the unshocked electrons of the pulsar wind (Takata et al. 2014). The result of the scattering of the UV photons with temperature $T = 10\,\mathrm{eV}$ on the cold relativistic electrons with Lorentz factor $\gamma = 10^4$ is shown in Figure 3 with a red dot-dashed line. The shift of the shock closer to the pulsar up to a distance $r = 5 \times 10^{10}$ cm (Takata et al. 2014) will lead to the increase of the magnetic field by a factor of two in comparison to the field strength discussed in the previous section if the magnetic field is dominated by that in the pulsar wind. The resulting synchrotron and inverse Compton emission from the shocked electrons generated in the region with $B = 80\,\mathrm{G}$ is shown in Figure 3 with black solid and dashed lines, respectively. The VERITAS upper limit clearly shows that the field in the region cannot be much smaller than 10 G (green lines in Figure 3). Thus, the VERITAS observations before and after the source-state change put limits on the minimum value of the magnetic field in a compact, synchrotron-emitting region, regardless of the precise mechanism of the charge acceleration or the source of the magnetic field.

We note that Papitto & Torres (2015) have proposed pulsar magnetic field threading of the accretion disk down to the corotation radius of PSR J1023+0038 (~24 km) as a field source for the synchrotron emission. Were this the case, the strength of the magnetic field could be much larger.

The VERITAS limits support the conclusion of the magnetically dominated pulsar wind discussed in Bogdanov et al. (2011). However, in both the MSP and accretion/LMXB states, there are alternative sources of magnetic fields that should be considered, namely, that of the companion in both cases and that of the accretion disk itself in the second case. Assuming that the companion is tidally locked, observations of rapidly rotating, low-mass stars suggest a surface magnetic field strength on the order of 1 kG (Morin 2012). The observed orbital variations may also indicate a strong, subsurface magnetic field in the companion (Archibald et al. 2013).

The authors are grateful to A. Archibald for providing a Jodrell Bank radio ephemeris for PSR J1023+0038, which made the analysis described in Section 3.3 possible.

This research is supported by grants from the U.S. Department of Energy Office of Science, the U.S. National Science Foundation, and the Smithsonian Institution, and by NSERC in Canada. We acknowledge the excellent work of the technical support staff at the Fred Lawrence Whipple Observatory and at the collaborating institutions in the construction and operation of the instrument. E.A. acknowledges support by the Spanish Ministerio de Economia y Competitividad (MINECO) under grants AYA2013-47447-C3-1-P. The VERITAS Collaboration is grateful to Trevor Weekes for his seminal contributions and leadership in the field of VHE gamma-ray astrophysics, which made this study possible.

Facility: VERITAS.

REFERENCES

Abramowski, A., Acero, F., Aharonian, F., et al. 2011, A&A, 531, L18
Acciari, V. A., Beilicke, M., Blaylock, G., et al. ApJ, 679, 1427
Aharonian, F., Akhperjanian, A. G., Aye, K. M., et al. 2005, A&A, 442, 1
Aharonian, F., Akhperjanian, A. G., Anton, G., et al. 2009, A&A, 499, 273
Aliu, E., Anderhub, H., Antonelli, L. A., et al. 2008, Sci, 322, 1221
Aliu, E., Arlen, T., Aune, T., et al. 2011, Sci, 334, 6052
Alpar, M. A., Cheng, A. F., Ruderman, M. A., & Shaham, J. 1982, Natur, 300, 728
Anderhub, H., Antonelli, L. A., Antoranz, P., et al. 2009, ApJ, 702, 266
Archibald, A. M., Bogdanov, S., Patruno, A., et al. 2014, arXiv:1412.1306
Archibald, A. M., Kaspi, V. M., Bogdanov, S., et al. 2010, ApJ, 722, 88
Archibald, A. M., Kaspi, V. M., Hessels, J. W. T., et al. 2013, arXiv:1311.5161
Archibald, A. M., Stairs, I. H., Ransom, S. M., et al. 2009, Sci, 324, 1411
Arons, J., & Tavani, M. 1993, ApJ, 403, 249
Bassa, C. G., Patruno, A., Hessels, J. W. T., et al. 2014, MNRAS, 441, 1825
Bednarek, W., & Sobczak, T. 2014, MNRAS, 445, 2842
Bogdanov, S. 2015, arXiv:1508.05844
Bogdanov, S., Archibald, A. M., Hessels, J. W. T., et al. 2011, ApJ, 742, 97
Corbel, S., Dubus, G., Tomsick, J. A., et al. 2012, MNRAS, 421, 2947
Coti Zelati, F., Baglio, M. C., Campana, S., et al. 2014, MNRAS, 444, 1783
Daniel, M. K. 2008, Proc. ICRC (Mexico City), 3, 1325
de Jager, O. C. 1989, A&A, 221, 180
de Jager, O. C. 1994, ApJ, 436, 239
Deller, A. T., Archibald, A. M., Brisken, W. F., et al. 2012, ApJL, 756, L25
Deller, A. T., Moldon, J., Miller-Jones, J. C. A., et al. 2015, ApJ, 809, 13
Espinoza, C. M., Guillemot, L., Çelik, Ö, et al. 2013, MNRAS, 430, 571
Fomin, V. P., Stepanian, A. A., Lamb, R. C., et al. 1994, APh, 2, 137
Halpern, J. P., Gaidos, E., Sheffield, A., Price-Whelan, A. M., & Bogdanov, S. 2013, ATel, 5514, 1

Hanna, D., McCann, A., McCutcheon, M., & Nikkinen, L. 2010, NIMPA, 612, 278
Harding, A. K., Usov, V. V., & Muslimov, A. G. 2005, ApJ, 622, 531
H.E.S.S. Collaboration, Abramowski, A., Acero, F., et al. 2013, A&A, 551, A94
Hillas, A. M. 1985, Proc. ICRC (La Jolla), 3, 445
Hobbs, G. B., Edwards, R. T., & Manchester, R. N. 2006, MNRAS, 369, 655
Hofmann, W., Jung, I., Konopelko, A., et al. 1999, APh, 12, 135
Holder, J., Atkins, R. W., Badran, H. M., et al. 2006, APh, 25, 391
Holder, J., Acciari, V. A., Aliu, E., et al. 2008, in AIP Conf. Ser. 1085, High Energy Gamma-Ray Astronomy, ed. F. A. Aharonian, W. Hofmann, & F. M. Rieger (Melville, NY: AIP), 657
Homer, L., Szkody, P., Chen, B., et al. 2006, AJ, 131, 562
Kieda, D. & VERITAS Collaboration 2013, arXiv:1308.4849
Kong, A. K. H. 2013, ATel, 5515, 1
Krawczynski, H., Carter-Lewis, D. A., Duke, C., et al. 2006, APh, 25, 380
Li, K. L., Kong, A. K. H., Takata, J., et al. 2014, ApJ, 797, 111
Li, T., & Ma, Y. 1983, ApJ, 272, 317
Longair, M. S. 2011, in High Energy Astrophysics, ed. S. L. Malcolm (Cambridge: Cambridge Univ. Press), 237
Malyshev, D., Zdziarski, A., & Chernyakova, M. 2013, MNRAS, 434, 2380
McCutcheon, M. W. 2012, PhD thesis, McGill University
McCutcheon, M. & for the VERITAS Collaboration 2009, arXiv:0907.4974
Morin, J. 2012, Low-mass Stars and the Transition Stars/Brown Dwarfs, ed. C. Reylé, (Les Ulis: EAS Publications Series), 57, 165
Otte, N. 2007, J. Instrum., 003
Papitto, A., Ferrigno, C., Bozzo, E., et al. 2013, Natur, 501, 517
Papitto, A., & Torres, D. F. 2015, ApJ, 807, 33
Patruno, A., Archiabld, A., Bogdanov, S., et al. 2013, ATel, 5516, 1
Ransom, S. M. 2008, in Dynamical Evolution of Dense Stellar Systems, Vol. 246, ed. E. Vesperini, M. Giersz, & A. Sills (Cambridge: Cambridge Univ. Press)
Ray, P. S., Abdo, A., Parent, D., et al. 2012, arXiv:1205.3089
Roberts, M. 2011, in AIP Conf. Ser. 1357, Radio Pulsars: An Astrophysical Key To Unlock The Secrets Of The Universe, ed. M. Burgay et al. (Melville, NY: AIP), 127
Rolke, W. A., Lopez, A. M., & Conrad, J. 2005, NIMPA, A551, 493
Roy, J., Ray, P. S., Bhattacharyya, B., et al. 2015, ApJL, 800, L12
Stappers, B. W., Archibald, A. M., Hessels, J. W. T., et al. 2014, ApJ, 790, 39
Stappers, B. W., Archibald, A., Bassa, C., et al. 2013, ATel, 5513, 1
Szkody, P., Fraser, O., Silvestri, N., et al. 2003, AJ, 126, 1499
Takata, J., Li, K. L., Leung, G. C. K., et al. 2014, ApJ, 785, 131
Tam, P. H. T., Hui, C. Y., Huang, R. H. H., et al. 2010, ApJL, 724, L207
Tavani, M., Arons, J., & Kaspi, V. 1994, ApJL, 433, L37
Tendulkar, S. P., Yang, C., An, H., et al. 2014, ApJ, 791, 77
Thorstensen, J., & Armstrong, E. 2005, AJ, 130, 759
Wex, N., Johnston, S., Manchester, R. N., et al. 1998, MNRAS, 298, 997